Chemiluminescence analyzer of NO_x as a high-throughput screening tool in selective catalytic reduction of NO

2011 Sci. Technol. Adv. Mater. 12 054211

(http://iopscience.iop.org/1468-6996/12/5/054211)

Sci. Technol. Adv. Mater. **12** (2011) 054211 (7pp) doi:10.1088/1468-6996/12/5/054211

Chemiluminescence analyzer of NO_x as a high-throughput screening tool in selective catalytic reduction of NO

Kwang Seok Oh[1] **and Seong Ihl Woo**

Department of Chemical and Biomolecular Engineering, Center for Ultramicrochemical Process Systems (CUPS) and Graduate school of EEWS (WCU), Korea Advanced Institute of Science and Technology, 373-1 Guseong-dong, Yuseong-gu, Daejeon 305-701, Republic of Korea

E-mail: siwoo@kaist.ac.kr

Received 16 June 2011
Accepted for publication 24 November 2011
Published 24 January 2012
Online at stacks.iop.org/STAM/12/054211

Abstract

A chemiluminescence-based analyzer of NO_x gas species has been applied for high-throughput screening of a library of catalytic materials. The applicability of the commercial NO_x analyzer as a rapid screening tool was evaluated using selective catalytic reduction of NO gas. A library of 60 binary alloys composed of Pt and Co, Zr, La, Ce, Fe or W on Al_2O_3 substrate was tested for the efficiency of NO_x removal using a home-built 64-channel parallel and sequential tubular reactor. The NO_x concentrations measured by the NO_x analyzer agreed well with the results obtained using micro gas chromatography for a reference catalyst consisting of 1 wt% Pt on γ-Al_2O_3. Most alloys showed high efficiency at 275 °C, which is typical of Pt-based catalysts for selective catalytic reduction of NO. The screening with NO_x analyzer allowed to select Pt-$Ce_{(X)}$ ($X = 1$–3) and Pt–$Fe_{(2)}$ as the optimal catalysts for NO_x removal: 73% NO_x conversion was achieved with the Pt–$Fe_{(2)}$ alloy, which was much better than the results for the reference catalyst and the other library alloys. This study demonstrates a sequential high-throughput method of practical evaluation of catalysts for the selective reduction of NO.

Keywords: chemiluminescence, NO_x, analyzer, high-throughput screening, selective catalytic reduction

1. Introduction

Nitrogen oxides, labeled as NO_x, are among the pollutants emitted during combustion in industrial boilers and automobiles. Efforts are being made at the regional and international levels to limit air pollution from the incineration and automobile industries [1–4]. Strict environmental regulations regarding air pollution are also being implemented in different parts of the world. Some of these regulations restrict NO_x emission levels for combustion processes. Concerning NO_x abatement from diesel engines, progress in high-throughput testing with parallel reactors allowed rapid screening of a large number of catalysts [5–8].

The ultimate goal of the combinatorial approach is to find the optimal catalyst composition with the minimum amount of research effort. In practice, this is accomplished by systematic and efficient exploration of the parameter space that controls the properties of the final products. The two keys to a successful combinatorial approach are the controlled synthesis of a collection of materials with systematic variations in structure and the subsequent high-throughput analysis of these materials. Speed, achieved through parallel synthesis and characterization, is therefore critical for the success of the combinatorial discovery process. The products of catalytic reactions can be analyzed with parallel or sequential measurements, using *in-situ* or post-reaction sampling. For several reasons, parallel screening is preferred for applications such as infrared thermography and laser-induced resonance-enhanced multiphoton ionization [9–14]. However,

[1] Present address: R&D Group Eco-Energy Team, Hyundai Engineering and Construction Co, LTD, 102-4 Mabuk-dong, Giheung-Gu, Yongin-Si, Gyeonggi-Do 446-716, Republic of Korea.

only temperature can be measured, and no chemical information is obtained on the gas generated in the reaction. Schüth and coworkers [15] demonstrated a new rapid-detection method based on color change of an organic dye in the presence of either educts or reaction products in reaction gas flow, under NO decomposition and NO reduction. While this technique is suitable for parallel screening, it has notable disadvantages. Particularly, each studied reaction requires selection of a specific dye, which is not always possible.

Sequential analysis of materials libraries is used when designing a parallel system is overly complicated or the total analysis time is not an issue. Sequential measurements often provide more detailed information about material properties than parallel methods. A number of analytical methods have been developed that are suitable for assessing NO_x emission and determination of low NO_x levels in the atmosphere. Chemiluminescence NO_x analyzers are usually used for continuous monitoring owing to their ease of access and handling. Most analytical tools used for selective catalytic reduction studies, including chemiluminescence NO_x analyzers, are not capable of resolving the processes occurring during short transient events. Nevertheless, they can be applied to gas analysis during the adsorption process as demonstrated in our previous study [16].

In this report, we present a novel high-throughput screening technique which uses a chemiluminescence NO_x analyzer. We have tested the validity of this method on a library of sixty Pt-based bimetallic catalysts supported on Al_2O_3 and carried out experiments on selective catalytic reduction of NO.

2. Experimental details

2.1. High-throughput synthesis of catalyst library

Creation of a catalyst library requires choosing the constituent elements and setting limits for the concentrations of individual elements and their sum. Based on the extensive literature on NO_x removal, we have previously selected four metals (Pt, Cu, Fe and Co), designed a 56-member library, and characterized its catalytic activity [8]. Building on those preliminary results, in this study we prepared a 60-member library of bimetallic catalysts supported on Al_2O_3, where one metal is Pt and another is Co, Zr, La, Ce, Fe or W. We label the members of the library as Pt-$M_{(X)}$, where X is the weight percentage of the alloyed metal M, whereas the Pt content was fixed at 1 wt%.

Using distilled water, we prepared six standard stock solutions of 0.025 M tetra-amine-platinum nitrate, 0.06 M cobalt nitrate, 0.04 M zirconyl nitrate, 0.025 M lanthanum nitrate, 0.025 M cerium nitrate, 0.065 M iron nitrate, and 0.017 M ammonium meta-tungstate. Each solution was distributed among 60 vials containing 50 mg of Al_2O_3 powder using a computer-controlled dispensing system (Chemspeed 2000 ASW, Chemspeed Technology). Relative concentrations of each component in the solution were adjusted so that the final catalyst powders contained 1 wt% of Pt and 1–10 wt% of another metal. After drying at 110 °C for 12 h the obtained catalyst powders were ground with a glass rod in the vials, manually transferred to cartridges, calcined in air, and reduced in a H_2 atmosphere at 500 °C for 4 h. Some cartridges were left

Table 1. Composition of the studied 60-member library.

Catalyst number	Loading (wt%)						
	Pt	Co	Zr	La	Ce	Fe	W
1	1	1	0	0	0	0	0
2	1	2	0	0	0	0	0
3	1	3	0	0	0	0	0
4	1	4	0	0	0	0	0
5	1	5	0	0	0	0	0
6	1	6	0	0	0	0	0
7	1	7	0	0	0	0	0
8	1	8	0	0	0	0	0
9	1	9	0	0	0	0	0
10	1	10	0	0	0	0	0
11	1	0	1	0	0	0	0
12	1	0	2	0	0	0	0
13	1	0	3	0	0	0	0
14	1	0	4	0	0	0	0
15	1	0	5	0	0	0	0
16	1	0	6	0	0	0	0
17	1	0	7	0	0	0	0
18	1	0	8	0	0	0	0
19	1	0	9	0	0	0	0
20	1	0	10	0	0	0	0
21	1	0	0	1	0	0	0
22	1	0	0	2	0	0	0
23	1	0	0	3	0	0	0
24	1	0	0	4	0	0	0
25	1	0	0	5	0	0	0
26	1	0	0	6	0	0	0
27	1	0	0	7	0	0	0
28	1	0	0	8	0	0	0
29	1	0	0	9	0	0	0
30	1	0	0	10	0	0	0
31	1	0	0	0	1	0	0
32	1	0	0	0	2	0	0
33	1	0	0	0	3	0	0
34	1	0	0	0	4	0	0
35	1	0	0	0	5	0	0
36	1	0	0	0	6	0	0
37	1	0	0	0	7	0	0
38	1	0	0	0	8	0	0
39	1	0	0	0	9	0	0
40	1	0	0	0	10	0	0
41	1	0	0	0	0	1	0
42	1	0	0	0	0	2	0
43	1	0	0	0	0	3	0
44	1	0	0	0	0	4	0
45	1	0	0	0	0	5	0
46	1	0	0	0	0	6	0
47	1	0	0	0	0	7	0
48	1	0	0	0	0	8	0
49	1	0	0	0	0	9	0
50	1	0	0	0	0	10	0
51	1	0	0	0	0	0	1
52	1	0	0	0	0	0	2
53	1	0	0	0	0	0	3
54	1	0	0	0	0	0	4
55	1	0	0	0	0	0	5
56	1	0	0	0	0	0	6
57	1	0	0	0	0	0	7
58	1	0	0	0	0	0	8
59	1	0	0	0	0	0	9
60	1	0	0	0	0	0	10

(a)

(b)

Figure 1. 64-Channel sequential and parallel tubular reactor system (a) front view and (b) inside view.

empty for background measurements and one cartridge was filled with the reference catalyst (1 wt% of Pt on γ-Al_2O_3). The composition of the 60-member catalyst library is shown in table 1.

2.2. Reaction system: 64-channel sequential and parallel tubular reactor

Figure 1 shows the computer-controlled 64-channel sequential and parallel tubular reactor, which was developed for low-temperature (<505 °C) catalytic reactions. This setup contains 64 vertically aligned channels that allow 64 different gas-phase reactions to occur in sequential and parallel modes. The reactor body has a diameter of 290 mm and a height of 150 mm and is made of stainless steel. For easy mounting and exact weighing, the catalyst powder is placed in a 20 mm-long stainless steel cartridge of 5 mm inner diameter (i.d.) and 8 mm outer diameter (o.d.); the cartridge is then inserted into the reactor body. Metal frits containing 2 μm pores in the bottom of each cartridge support the catalyst powder. A capillary (1.6 mm o.d., 0.12 mm i.d., 500 mm length) connects the 16-port two-position valve and the inlet of each reactor. It dampens the effect of different pressure drops over the catalyst beds, thereby allowing to keep the same flow rate in each reactor channel within 1 ml min^{-1} (see table 2).

Table 2. Measured flow rates through individual reactor channels at a nominal applied He flow rate of 20.5 ml min^{-1}.

Channel number	Flow rate (ml min^{-1})	Channel number	Flow rate (ml min^{-1})	Channel number	Flow rate (ml min^{-1})
1	20.4	23	19.6	45	19.8
2	20.3	24	20.4	46	19.8
3	20.2	25	19.7	47	19.9
4	20.2	26	19.8	48	19.8
5	19.7	27	19.7	49	19.7
6	19.4	28	19.7	50	19.8
7	20.4	29	19.8	51	19.5
8	19.6	30	19.5	52	20.0
9	19.3	31	19.4	53	20.4
10	20.0	32	20.3	54	20.0
11	19.3	33	20.0	55	19.5
12	19.7	34	19.5	56	19.9
13	20.2	35	20.4	57	20.3
14	19.5	36	20.5	58	19.8
15	19.9	37	19.5	59	20.4
16	19.7	38	19.6	60	19.4
17	19.3	39	20.0	61	19.5
18	19.7	40	19.5	62	19.9
19	20.2	41	20.4	63	20.3
20	19.5	42	20.5	64	19.8
21	19.9	43	19.5		
22	19.7	44	19.6		

The reaction temperature is maintained by several independent temperature controllers, which receive feedback from thermocouples placed on the reactor body. The preheated reactant can be introduced sequentially from the top to each reactor channel. When the reactant gas is flown through one of the channels, helium gas is passed through the others to avoid catalyst oxidation by the air during the reaction step. A detailed description of the setup can be found in [8].

In this work, 20 mg of catalyst was placed in each reactor channel and heated under a helium gas flow at 200 °C for activation. The catalysts were then exposed to a gas mixture of 2000 ppm NO, 2700 ppm C_3H_6, 3.2 vol.% O_2, and helium balance. The reactions were carried out at temperatures of 250, 275, 300, 350 and 400 °C and the gas flow rate in each channel was ~20 ml min^{-1}.

The product gas was analyzed by a commercial NO_x analyzer (Model 42H, Thermo Environmental Instrument) combined with a micro gas chromatograph (GC, Agilent 3000). The analyzer detects chemiluminescence generated by the reaction of NO with ozone, which is produced within the instrument in a discharge tube. It allows quantitative detection of NO at levels as low as 1 part per million (ppm) in ambient air drawn in at flow rates of 200–300 ml min^{-1}. To avoid errors

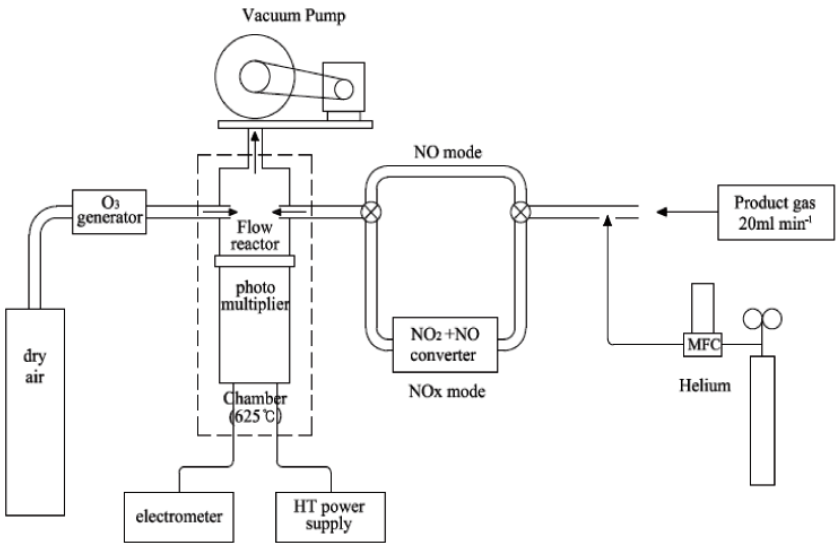

Figure 2. Schematic of the chemiluminescence NO_x analyzer.

Table 3. Reading of the NO_x analyzer at the nominal inlet NO concentration of 2000 ppm and different He flow rates.

Helium flow rate ($ml\,min^{-1}$)	Analyzer reading (ppm)
150	2254
200	2131
250	1992
300	1855
350	1723

caused by water in the converter of the NO/NO_x analyzer, a water trap containing molecular sieves was installed in front of the sample inlet of the analyzer.

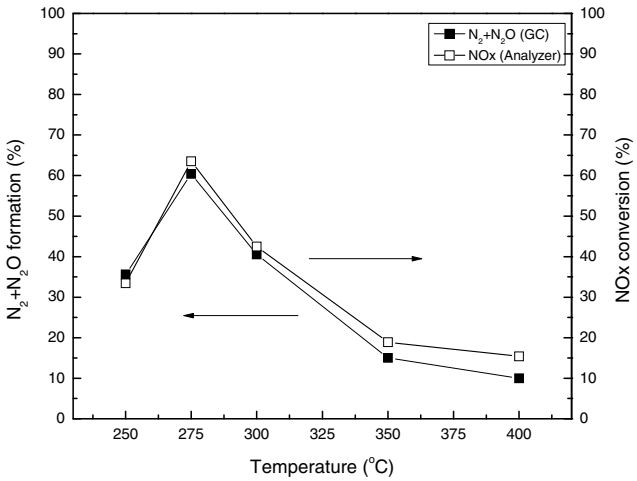

Figure 3. Comparison of the gas chromatography and NO_x analyzer results for selective catalytic reduction of NO with the reference Pt/Al_2O_3 catalyst at different temperatures.

3. Results and discussion

3.1. Optimization of gas flow rate in the NO_x analyzer for calibration

The NO_x analyzer is designed to measure NO_x levels in ambient air, and the elements of a typical analyzer are shown in figure 2. The core of the instrument is the low-pressure reaction chamber where the chemiluminescence reaction occurs. Air is passed through an ozone generator and the partially ozonized air is then metered into the chamber where it reacts with the nitric oxide in the sample gas. When the analyzer and vacuum pump (intake air) are turned on, the reading from the manufacturer's air flow meter indicates the air intake at a presumably optimal flow rate of approximately $350\,ml\,min^{-1}$. At this flow rate and pressure, the instrument has minimal output fluctuations with variations in flow rate and pressure. Note that at our reaction conditions, the low flow rate ($20\,ml\,min^{-1}$) might damage the reaction chamber of the instrument because of high temperature (625 °C), thereby degrading the instrument performance.

To optimize air flow, we first measured the additional helium flow rate by reading the post-attachment flow rate registered on the air flow meter of the analyzer. As shown in table 3, at low flow rates, the reading of the NO_x analyzer was higher than expected, indicating some suck-in effect. At high flow rates, the reading was lower than expected, indicating flow obstruction and pressure build up [17]. At helium flow rates close to $250\,ml\,min^{-1}$, the flow meter of the analyzer after attachment showed $350\,ml\,min^{-1}$. This reading is consistent with a value expected for a flow meter which was calibrated for air and exposed to a helium flow of $250\,ml\,min^{-1}$. Thus, we selected this flow rate for our experiments and found it optimal when the instrument was connected with the product gas outlet. Prior to the experiment, the reading was zeroed, and concentration calibration was performed using a standard gas mixture of 2000 ppm NO and 500 ppm NO_2. The NO and NO_x span values were set to predetermined values and not changed thereafter. We used the NO_x reading (total $NO + NO_2$) so that any NO_2 formed in the system by reaction of NO with oxygen contamination

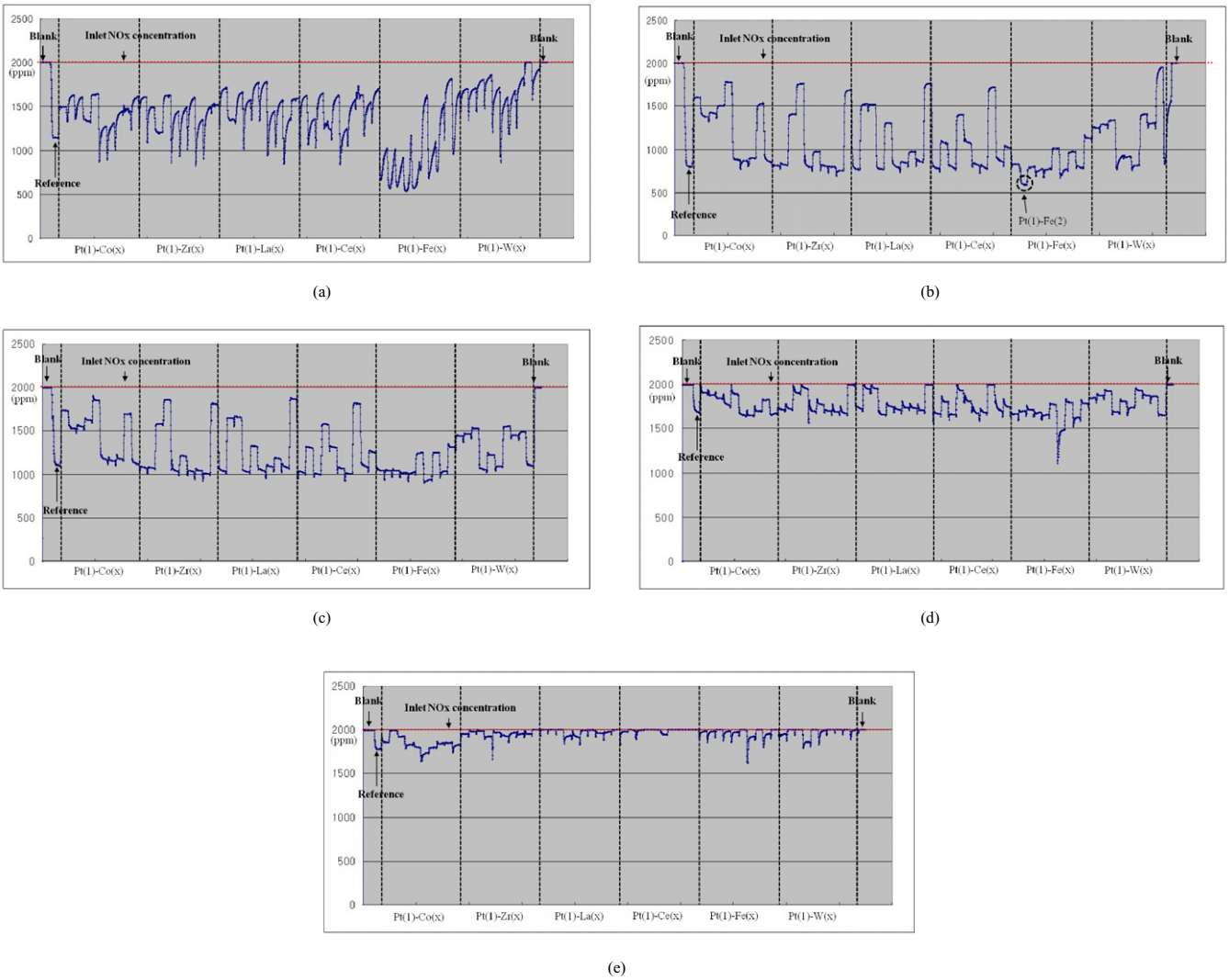

Figure 4. Time traces of the NO_x analyzer signal for different catalysts tested at (a) 250, (b) 275, (c) 300, (d) 350 and (e) 400 °C.

could also be measured as NO by reconversion in the catalytic converter of the instrument.

3.2. Catalytic activity test of 60-member library

The reactivity of the 60-member catalyst library was evaluated and effluent gases from high-throughput screening reactors were sequentially analyzed by the NO_x analyzer combined with the micro GC. Three channels were left empty (#1, 63, 64) for background test and one channel (#2) was filled with the reference catalyst. To evaluate the accuracy of this method, we compared the NO_x conversion to N_2O and N_2 measured by the micro GC and the chemiluminescence NO_x analyzer, as shown in figure 3. The maximum NO conversions measured by the NO_x analyzer and GC are, respectively, 64 and 60% at 275 °C. Traa *et al* [18] reported that above the temperature associated with maximum NO_x reduction, a considerable amount of NO_2 was present in the reactor effluent. Therefore, although the difference of NO_x conversion among the two analysis methods slightly increased above 275 °C, mainly due to NO_2 formation, we conclude that the NO_x concentrations measured by the NO_x analyzer and micro GC agreed well.

Figure 4 shows typical raw data acquired by the NO_x analyzer during the reaction. Periodic oscillations are observed for all reaction temperatures. Several authors have reported oscillations of the NO_x concentration at certain conditions during hydrocarbon-selective catalytic reduction (HC-SCR) [19–21]. They stressed the complex nature of the HC-SCR system, which can be very sensitive to small changes in the reaction conditions induced by the presence of 10% water during selective reduction of C_2H_4 on Pt/ZSM-5 catalyst. However, the oscillation seen in figure 4 is associated with transient fluctuation of the reactant gas flow rate; specifically, it is caused by the sequential switching of the 16-port two-position valve from reactor channel #1 to 64 with an interval of 3 min. This oscillation enabled us to clarify the catalytic performance of each catalyst. As can be seen in figure 4, NO_x concentrations of blank channels are maintained at 2000 ppm at all reaction temperatures and the minimum NO_x concentration for the reference catalyst is observed at 275 °C, indicating maximum NO_x conversion. The overall catalytic activity of the library increases until 275 °C, and then declines drastically with increasing temperature, resulting in less than 5% NO_x conversion at 400 °C.

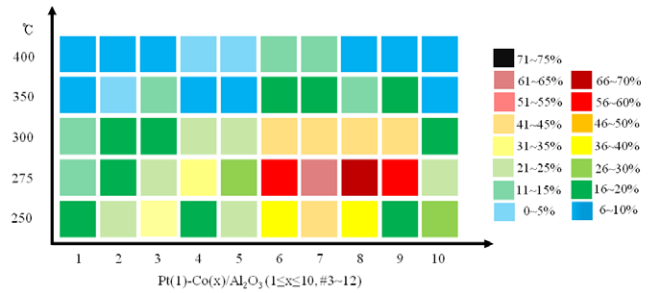

Figure 5. NO_x conversion efficiency of Pt–$Co_{(X)}$ catalysts (#3–12) as a function of temperature and Co content X (wt%).

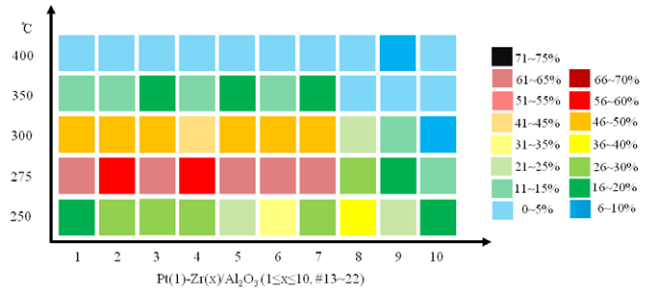

Figure 6. NO_x conversion efficiency of Pt–$Zr_{(X)}$ catalysts (#13–22) as a function of temperature and Zr content X (wt%).

Figure 5 shows the catalytic performance of the Pt–$Co_{(X)}$ catalyst as a function of temperature and the Co content X. Pt–$Co_{(8)}$ shows a maximum of 66% NO_x conversion at 275 °C, which is greater than that of the reference catalyst (60%). With increasing Co loading from 1 to 8 wt%, NO_x reduction increases and the operational temperature window widens compared with the reference. However, the catalytic performance degrades at $X = 9$ and 10 wt%, indicating that excess Co doped the active Pt particles, reducing the density of active sites on the catalysts [22].

Figure 6 shows results of NO_x reduction on Pt–$Zr_{(X)}$ catalyst as a function of temperature and Zr content X. The activity peaks at 275 °C and is very similar for $X =$ 1–7 wt%, with a slightly higher NO_x conversion (62%) for $X = 7$ wt%. At higher Zr loading the catalytic performance decreases and the optimal temperature shifts to 250 °C. This observation can be explained by the relationship between the NO_x reduction and propylene oxidation (not shown), which is largely responsible for the NO_x conversion with Pt-based catalysts promoted by additives [23]. As the loading of metal additives such as W, Mo, V, Ga or Zr is increased, the catalytic activity increases and the propylene oxidation occurs at lower temperatures [24–26]. However, the catalytic efficiency of Pt–$Zr_{(X)}$ ($X =$ 8–10 wt%) catalysts decreases from 62 to 40%, in contrast with results reported in the literature, indicating that excess Zr loading reduced the Pt dispersion.

Figure 7 shows the activities of Pt–$La_{(X)}$ catalysts. The NO_x conversion peaks at 275 °C for $X =$ 1–7 wt%, with a maximum of 67% conversion observed for $X = 4$. The conversion value decreases at larger X, and its temperature maximum shifts to 250 °C for $X =$ 8–10 wt%, similar to results of figure 6.

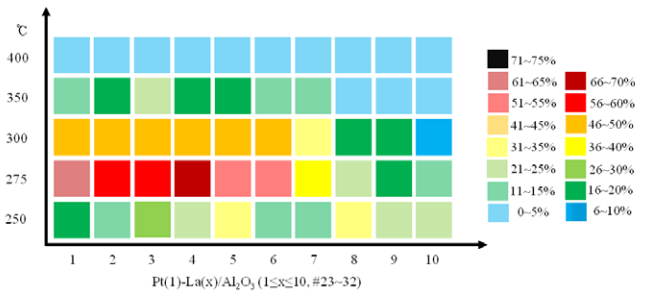

Figure 7. NO_x conversion efficiency of Pt–$La_{(X)}$ catalysts (#23–32) as a function of temperature and La content X (wt%).

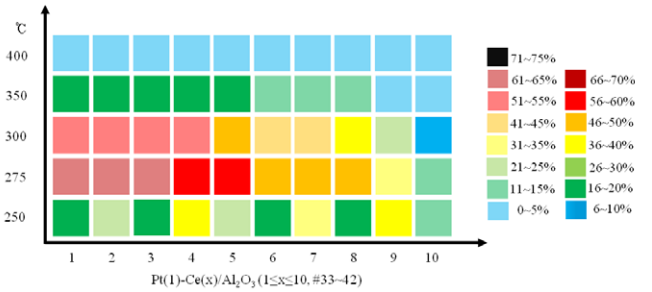

Figure 8. NO_x conversion efficiency of Pt–$Ce_{(X)}$ catalysts (#33–42) as a function of temperature and Ce content X (wt%).

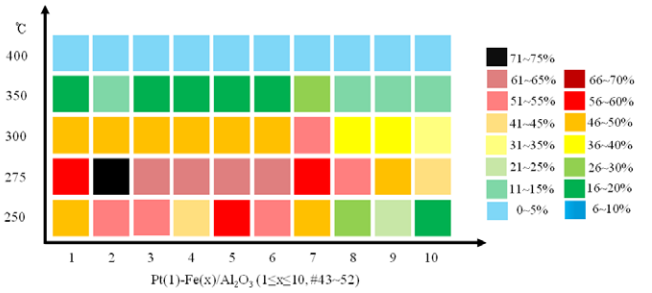

Figure 9. NO_x conversion efficiency of Pt–$Fe_{(X)}$ catalysts (#43–52) as a function of temperature and Fe content X (wt%).

We found that addition of Ce strongly affects the NO_x reduction, as shown in figure 8. About 60% NO_x conversion is obtained with Pt–$Ce_{(X)}$ ($X =$ 1–3) catalysts at 275 °C, with the conversion rate decreasing at higher temperatures. When compared with the reference catalyst, the NO_x reduction activity of Pt–$Ce_{(X)}$ ($X =$ 1–3) is the same at 275 °C and is significantly higher at 300 °C; the activity value at 300 °C (54%) is also higher than the values measured for the Co, Zr, La, Fe or W-containing catalysts at the same temperature. It was reported that CeO_2 can be attributed to its higher reducibility in the presence of Pt, the higher dispersion of Pt over CeO_2, and resistance to coke deposition due to oxygen storage-release capability [27]. Hence, it seems that the high NO_x conversion shown at 300 °C is mainly due to the effect of Ce promotion, resulting in a wide temperature window.

The effect of metal addition to Pt/Al_2O_3 catalyst is especially pronounced for Pt–$Fe_{(X)}$ alloys, as can be seen in figure 9. NO_x reduction is maximal at 275 °C for any Fe content, and for $X =$ 1–7 wt% the catalytic efficiency is higher than for Co, Zr, La, Ce or W-containing catalysts, with the

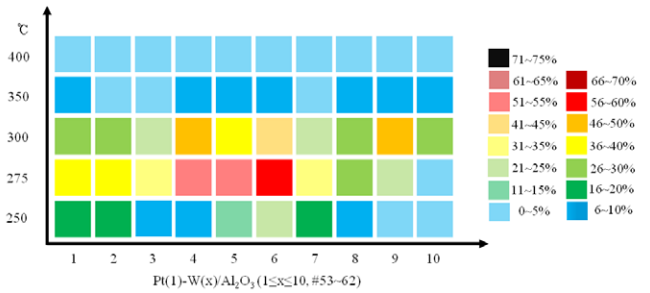

Figure 10. NO_x conversion efficiency of Pt–$W_{(X)}$ catalysts (#53–62) as a function of temperature and W content X (wt%).

values of 44–58% at 250 °C and 47–53% at 300 °C. Pt–$Fe_{(2)}$ alloy shows the highest efficiency (71%) among all the 60 catalysts studied. The NO reduction efficiency of Pt–Fe alloys was higher than that of Pt reference after H_2 pretreatment and lower after oxidizing pretreatment. In addition, Pt particles were found to react with Fe additives to form homogeneous Pt–Fe alloy particles on Al_2O_3 under reducing conditions. Meanwhile, Pt–Fe alloy particles segregated into Pt and Fe_2O_3 and formed a Fe_2O_3 layer on the Pt particles, hindering their reaction with NO [28]. Therefore, we attribute the enhanced catalytic performance of Pt–Fe alloys to their homogeneity and the pretreatment in H_2 atmosphere. The effect of Fe addition to the Pt/Al_2O_3 catalyst was also reported by Tanaka *et al* [29] for CO oxidation in H_2.

The addition of W to Pt had little effect on the catalytic activity as shown in figure 10. The maximum NO_x conversion efficiency decreased from 60% for Pt to 57% for Pt–$W_{(6)}$, which shows the best performance among the ten Pt–W catalysts at 275 °C. The catalytic activity decreased significantly at higher temperatures.

4. Conclusions

We have prepared a library of 60 binary alloys containing Pt and Co, Zr, La, Ce, Fe or W and tested it for selective catalytic reduction of NO using a home-built 64-channel parallel and sequential tubular reactor. High-throughput, time-resolved measurements were realized using a commercial chemiluminescence analyzer of NO_x, and the entire library was screened within 2.5 h. The Pt–$Ce_{(X)}$ ($X = 1$–3) and Pt–$Fe_{(2)}$ alloys showed high NO_x conversion efficiency at 275 °C and a wide reaction temperature window as compared with the reference Pt catalyst. The catalytic activity of these alloys requires a further study.

Acknowledgment

This work was supported by the Korea Science and Engineering Foundation (KOSEF) grant (WCU program, 31-2008-000-10055-0) funded by the Ministry of Education and Science and Technology (MEST).

References

[1] Komazaki Y, Shimizu H and Tanaka S 1999 *Atmos. Environ.* **33** 4363
[2] Alvarez R, Weilenmann M and Favez J Y 2008 *Atmos. Environ.* **42** 4699
[3] Oh K S and Woo S I 2006 *Catal. Lett.* **110** 247
[4] Oh K S and Woo S I 2007 *Appl. Surf. Sci.* **254** 677
[5] Krantz K, Ozturk S and Senkan S 2000 *Catal. Today* **62** 281
[6] Ozturk S and Senkan S 2002 *Appl. Catal.* A **38** 243
[7] Richter M, Langpape M, Kolf S, Grubert G, Eckelt R, Radnik J, Schneider M, Paul M M and Fricke R 2002 *Appl. Catal.* B **36** 261
[8] Oh K S, Park Y K and Woo S I 2005 *Rev. Sci. Instrum.* **76** 062219
[9] Hagemeyer A, Jandeleit B, Liu Y, Poojary D M, Turner H W, Volfe F Jr and Weinberg W H 2001 *Appl. Catal.* A **221** 23
[10] Holzwarth A, Schmidt H W and Maier W F 1998 *Angew. Chem., Int. Ed. Engl.* **37** 2644
[11] Reetz M, Becker M H, Kuhling K M and Holzwarth A 1998 *Angew. Chem., Int. Ed. Engl.* **37** 2647
[12] Moates F C, Somani M, Annamalai J, Richardson J T, Luss D and Wilson R C 1996 *Ind. Eng. Chem. Res.* **35** 4801
[13] Taylor S J and Morken J P 1998 *Science* **280** 267
[14] Senkan S 1998 *Nature* **394** 350
[15] Busch O M, Hoffmann C, Johann T R F, Schmidt H W, Strehlau W and Schüth F 2002 *J. Am. Chem. Soc.* **124** 13527
[16] Oh K S and Woo S I 2007 *Appl. Surf. Sci.* **254** 677
[17] Pai T G, Payne W J and Legall J 1987 *Anal. Biochem.* **166** 150
[18] Traa Y, Burger B and Weitkamp J 1999 *Mircopor. Mesopor. Mater.* **30** 3
[19] Halasz I, Brenner A, Shelef M and Simon Ng K Y 1995 *J. Phys. Chem.* **99** 17186
[20] Cho B K, Yie J E and Rahmoeller K M 1995 *J. Catal.* **157** 14
[21] Traa Y, Breuninger M, Burger B and Weitkamp J 1997 *Angew. Chem., Int. Ed. Engl.* **36** 2113
[22] Ishibashi K, Matsumoto S, Ishibashi K, Yokota K, Kondo S, Sekizawa K and Kasahara S 1992 *JP 4197422 A*
[23] Burch R and Milington P J 1995 *Catal. Today* **26** 185
[24] Dawody J, Skoglundh M and Fridell E 2004 *J. Mol. Catal.* A **209** 215
[25] Kikuyama S, Matsukuma I, Kikuchi R, Sasaki K and Eguchi K 2002 *Appl. Catal.* A **226** 23
[26] Salem I, Courtois X, Corbos E C, Marecot P and Duprez D 2008 *Catal. Commun.* **9** 664
[27] Trovarelli A 1996 *Catal. Rev. Sci. Eng.* **38** 439
[28] Sakamoto Y, Higuchi K, Takahashi N, Yokota K, Doi H and Sugiura M 1999 *Appl. Catal.* B **23** 159
[29] Tanaka T *et al* 2004 *Catal. Lett.* **92** 115